Liquid Crystals
Publication details, including instructions for authors and subscription information:
http://www.informaworld.com/smpp/title~content=t713926090

Evidence for three typical behaviours of the helicity in the SmC_{alpha}* phase from recent benzoate ester series

Valerie Laux; Noel Isaert; Valerie Faye; Huu Tinh Nguyen

Online publication date: 06 August 2010

To cite this Article Laux, Valerie , Isaert, Noel , Faye, Valerie and Nguyen, Huu Tinh(2000) 'Evidence for three typical behaviours of the helicity in the SmC_{alpha}* phase from recent benzoate ester series', Liquid Crystals, 27: 1, 81 — 88
To link to this Article: DOI: 10.1080/026782900203254
URL: http://dx.doi.org/10.1080/026782900203254

LIQUID CRYSTALS, 2000, VOL. 27, NO. 1, 81–88

Evidence for three typical behaviours of the helicity in the SmC^*_α phase from recent benzoate ester series

VALERIE LAUX*

Laboratoire de Thermophysique de la Matière Condensée, UPRESA CNRS 8024, MREID, Université du Littoral Côte d'Opale, 145 Avenue Maurice Schumann, 59140 Dunkerque, France

NOEL ISAERT

Laboratoire de Dynamique et Structure des Matériaux Moléculaires, UPRESA CNRS 8024, Bâtiment P5, Université de Lille I, 59655 Villeneuve d'Ascq, France

VALERIE FAYE and HUU TINH NGUYEN

Centre de Recherche Paul Pascal, CNRS, Avenue A. Schweitzer, 33600 Pessac, France

(*Received 3 April 1999; accepted 8 August 1999*)

We have studied by optical means recently synthesized benzoate ester series exhibiting SmC^*_A, SmC^*_{FI}, SmC* and SmC^*_α phases. We have made pitch measurements on SmC^*_A and SmC* phases, using the Grandjean–Cano method, and optical period measurements on the SmC^*_α phase, on free surface drops. The results are in good agreement with the pitch and optical period evolutions we previously described for other compounds—especially those of a thiobenzoate series. We have also shown that one of the structural models proposed in the literature is in agreement with our experimental results, and have established a qualitative relation between optical period measurements, the azimuthal difference between two successive layers, and the helical pitch. We present results for several benzoate compounds, using a new classification of the observed behaviours.

1. Introduction

Since the antiferroelectric liquid crystal material MHPOBC was discovered, numerous chiral compounds presenting SmC^*_A, SmC*, SmC^*_{FI} and especially SmC^*_α phases have been synthesized. Many experimental studies concerning the SmC^*_α phase have been made and reported in the literature, but the results have not allowed determination of the phase structure. In particular, no result has been obtained by optical observation, and the SmC^*_α phase could not be distinguished optically from the SmA phase.

We have previously studied the SmC^*_α phase by optical means with the purpose of identifying a special texture, and to obtain evidence for some particular optical phenomena. We first worked on five compounds of a thiobenzoate series [1]. We observed on free surface drops periodic ellipticity fringes, the so-called Friedel fringes; these fringes were the first direct observation of a helical structure in the SmC^*_α phase [2, 3]. We were also able to measure the fringe period as a function of temperature [3]. We performed a complete study of this optical period and obtained evidence for different period behaviours, depending on the thermal history of the sample or on the phase sequence of the compound. We showed throughout that these different behaviours are always part of a general behaviour, typical of the SmC^*_α phase. We compared this general behaviour with structural models proposed in the literature, concluding that the model proposed by Zeks and Cepic [4, 5] seems to be in good agreement with our experimental results. According to this model, the tilt angle of the molecules is constant through all the layers, the phase difference α between two nearest layers is also constant, and the helicoidal modulation extends over only a few layers. The phase difference α is rather significant, and can change from 0 to π, crossing $\pi/2$, when interactions between nearest and next nearest layers change. This study has been reported recently [6].

* Author for correspondence; e-mail: laux@univ-littoral.fr

Liquid Crystals ISSN 0267-8292 print/ISSN 1366-5855 online © 2000 Taylor & Francis Ltd
http://www.tandf.co.uk/journals/tf/02678292.html

To verify our earlier observations and measurements obtained on only one series and five compounds, we then performed an experimental study on a large number of compounds belonging to different series [7–9]. We studied in particular several compounds from four benzoate series, using the same experimental methods as for the thiobenzoate series. We again observed the general behaviour previously determined: as for the thiobenzoate series, this can be displayed completely or only partly. The large number of compounds studied also allowed us to devise a new classification made up of three categories based on the phase sequence and on the pitch evolution in the SmC* phase. Our measurements are in good agreement with the first study, and show that the SmC^*_α phase always exhibits the same behaviour, whatever the general formula of the liquid crystal material.

In this paper we present the compounds used for this study, and remind the reader succinctly of the methods used to measure the helical pitch and the fringe period. Both methods have been precisely described in the paper concerning the thiobenzoate series [6]. We then report the experimental results using the new classification. In the discussion, we confirm that the structural model proposed by Zeks and Cepic fits conveniently with our experimental results, and we correlate the optical period evolution with the azimuthal angle variations.

2. Compounds and experimental techniques

2.1. *The benzoate series*

We have studied several compounds belonging to benzoate ester series which have already been reported [10]. The general formula is the following:

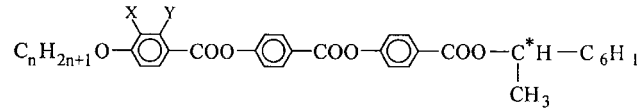

X = *Y* = *H* *n*HHBBM7 (*n*HH series), where *n* = 7 to 12;
X = *F*, *Y* = *H* *n*FHBBM7 (*n*FH series), where *n* = 8 to 12;
X = *H*, *Y* = *F* *n*HFBBM7 (*n*HF series), where *n* = 8 to 12;
X = *Y* = *F* *n*FFBBM7 (*n*FF series), where *n* = 8 to 12.

Tables 1 to 4 display the transition temperatures and enthalpies obtained by DSC for each series [10]. The most complete sequence exhibits six mesophases: SmC^*_A–SmC^*_{FI1}–SmC^*_{FI2}–SmC*–SmC^*_α–SmA. All these

Table 1. Transition temperatures (°C) and enthalpies (kJ mol^{-1}) (in italics) for the *n*HH series (positive enthalpy values are given for the heating scans; negative values for cooling scans). Parentheses denote a monotropic transition.

n	Cr	SmC^*_A	SmC^*_{FI1}	SmC^*_{FI2}	SmC*	SmC^*_α	SmA	I
7	•	82.8	—	—	—	•	(69.8)	•	(72.6)	•	141.9	•
		30.8							*− 0.023*[a]		*− 5.73*	
8	•	89.05	•	(58.4)	•	(74.5)	•	(87.8)	•	90.8	•	94.4	•	139.7	•
		34.7		*− 0.003*		?		*− 0.003*				*− 0.47*[a]		*− 5.51*	
9	•	95.8	•	(90.1)	•	(92.2)	•	97.2	•	106.6	•	109.2	•	136.0	•
		38.6		*− 0.009*		*− 0.002*		*− 0.009*				*− 0.14*[a]		*− 5.36*	
10	•	90.3	•	99.2	•	100.6	•	102.7	•	114.3	•	115.3	•	135.5	•
		34.5		*− 0.006*		*− 0.002*		*− 0.016*				*− 0.252*[a]		*− 5.23*	
11	•	82.5	•	86.2	•	90.8	•	92.7	•	117.4	—		•	131.4	•
		34.4						*− 0.010*		*− 0.160*				*− 5.08*	
12	•	72.0	•	85.6	•	87.5	•	92.3	•	119.2	—		•	131.5	•
		34.9								*− 0.290*				*− 5.30*	

[a] Sum of transition enthalpies.

Table 2. Transition temperatures (°C) and enthalpies (kJ mol^{-1}) (in italics) for the *n*FH series (positive enthalpy values are given for the heating scans; negative values for cooling scans). Parentheses denote a monotropic transition.

n	Cr	SmC^*_A	SmC^*_{FI1}	SmC^*_{FI2}	SmC*	SmC^*_α	SmA	I
8	•	87.4	•	91.5	•	97.0	—		—	•	100.4	•	132.5	•
		37.4		*− 0.008*		*− 0.01*	*− 0.10*				*− 0.037*[a]		*− 5.37*	
9	•	97.6	•	(95.8)	•	98.9	—	•	108.5	•	109.7	•	128.4	•
		43.7		*− 0.008*		*− 0.018*					*− 0.222*[a]		*− 5.38*	
10	•	89.3	•	101.8	•	103.4	—	•	112.8	•	113.3	•	127.1	•
		37.8		*− 0.013*		*− 0.029*					*− 0.243*[a]		*− 5.04*	
11	•	82.0	•	85.2	•	89.8	—	•	114.3	–		•	124.6	•
		36.9		*− 0.003*		*− 0.012*			*− 0.374*				*− 4.86*	
12	•	80.6	•	93.2	•	94.9	—	•	115.5	–		•	123.0	•
		37.7				*− 0.043*[a]			*− 0.480*				*− 4.62*	

[a] Sum of transition enthalpies.

Table 3. Transition temperatures (°C) and enthalpies (kJ mol^{-1}) (in italics) for the *n*HF series (positive enthalpy values are given for the heating scans; negative values for cooling scans). Parentheses denote a monotropic transition.

n	Cr		SmC^*_A		SmC^*_{FI1}		SmC^*_{FI2}	SmC*		SmC^*_α		SmA		I
8	•	57.6	—		—		—	—		—		•	126.4	•
		24.03											*− 5.53*	
9	•	75.5	—		—		—	•	(53.9)	•	(65.3)	•	123.1	•
		26.6							*− 0.002*		*− 0.004*		*− 5.34*	
10	•	75.6	—		—		—	•	(73.6)	•	84.1	•	122.6	•
		23.3							*− 0.002*		*− 0.007*		*− 5.49*	
11	•	75.2	—		—		—	•	92.5	•	95.8	•	120.3	•
		29.9							*− 0.008*		*− 0.030*		*− 5.42*	
12	•	66.3	•	(43.7)	•	73.3	—	•	98.9	•	100.8	•	118.9	•
		41.6							*− 0.006*		*− 0.027*		*− 5.48*	

Table 4. Transition temperatures (°C) and enthalpies (kJ mol^{-1}) (in italics) for the *n*FF series (positive enthalpy values are given for the heating scans; negative values for cooling scans. Parentheses denote a monotropic transition.

n	Cr		SmC^*_A		SmC^*_{FI1}		SmC^*_{FI2}		SmC*		SmC^*_α		SmA		I
8	•	72.2	—		—		—		—	•	(59.2)	•	135.7	•
		26.7									*− 0.006*		*− 5.33*	
9	•	71.1	•	76.8	•	79.2	•	84.7	• 89.3	•	94.5	•	131.8	•
		28.1		*− 0.001*		*− 0.001*		*− 0.006*	*− 0.007*		*− 0.026*		*− 5.13*	
10	•	56.1	•	91.2	•	92.7	•	95.0	• 100.8	•	103.5	•	130.3	•
		24.6		*− 0.011*		*− 0.003*		*− 0.010*	*− 0.011*		*− 0.004*		*− 5.18*	
11	•	58.8	•	70.5	•	71.4	•	80.5	• 108.6	•	109.5	•	127.7	•
		25.6						*− 0.008*			*− 0.174*[a]		*− 5.02*	
12	•	62.8	•	89.6	•	92.5	—		• 112.0	•	112.4	•	126.2	•
		36.0				*− 0.015*[a]					*− 0.264*[a]		*− 4.69*	

[a] Sum of transition enthalpies.

phases occur for the *n*HH and *n*FF series, except for a few homologues: 7HH does not exhibit SmC^*_A or SmC^*_{FI}, 11 and 12 HH do not exhibit the SmC^*_α phase. 8FF exhibits only SmC^*_α and SmA, 12FF does not exhibit the SmC^*_{FI2} phase.

The SmC^*_{FI2} phase does not appear in the *n*FH series; 8FH does not exhibit the SmC* phase, and 11 and 12 FH do not exhibit SmC^*_α.

The *n*HF series displays a rather reduced polymorphism: only the 12HF compound exhibits the complete sequence, except for the SmC^*_{FI2} phase; 9, 10 and 11HF display only SmC*, SmC^*_α and SmA. SmC* is monotropic for 9HF and 10HF, and SmC^*_α is monotropic for the 9HF compound. 8FH exhibits only the SmA phase.

For our study, these series are most interesting as the SmC^*_α phase appears generally over a large temperature range. The largest range is obtained for the 9 and 10HF compounds, and is about 11°C.

This study shows that the *n*HH and *n*FF series exhibit the same phase sequences, and the same behaviours in the SmC* and SmC^*_α phases. We thus report results for compounds belonging to the *n*HF, *n*FH and *n*FF series, and more precisely for 12HF, 8FH, 9FF, 10FF and 10FH.

2.2. *Experimental procedures*

To characterize these compounds, we performed pitch measurements on the SmC^*_A and SmC* phases, and optical period measurements on SmC^*_α. Samples were placed in a Mettler FP5 hot stage, and observed using an Ortholux Leitz polarizing microscope in the reflection mode.

To perform the helical pitch measurements, we used the Grandjean–Cano method [2, 6]. The liquid crystal is introduced into a prismatic cell made of two glass slides; a step lattice, produced by edge dislocations then appears. The lattice period is equal to one half the pitch in the SmC^*_A phase, and one full pitch in the SmC* phase. If the pitch range allows it, selective reflection colours are visible: $\lambda = np$ for the SmC^*_A phase, $\lambda = np$ and $\lambda = 2np$ for the SmC* phase (where λ is the reflected wavelength, n the average refractive index ($n \approx 1.5$) and p the pitch value).

On SmC^*_α we made observations on free surface drops [2, 3, 6]. When the phase studied is helical, this kind of sample displays Friedel fringes. Observing for the first time these fringes for the SmC^*_α phase [3], we obtained evidence for its helical structure; we also measured the fringe period versus temperature, and obtained a relation

between the period evolution and the phase structure. For a weak phase difference α, the optical period is equal to half the pitch. If α is close to $\pi/2$, the optical period becomes very important, and exhibits a divergence when $\alpha = \pi/2$ [6].

Both methods were applied to the above liquid crystal materials; details of the methods have been previously reported [3, 6].

3. Experimental results

The results obtained for the new benzoate ester series studied are in agreement with those previously obtained for a thiobenzoate series [6] and for chiral non-symmetric dimesogens [7, 8]. The optical period in the SmC^*_α phase can evolve differently, depending on the compound or on the sample thermal history [6]. We also noticed that this evolution depends on the liquid crystal phase sequence and on the pitch variations in the SmC* phase.

We shall now report results for the different benzoate series: the study of numerous compounds allowed us to identify three categories, determined by the phase sequence and the pitch variations in the SmC* phase. All the compounds studied follow this classification, except for one which exhibits an unusual phase sequence. We think it is better to describe the fringe movements and the precise optical period evolution in SmC^*_α only for the first category considered; after that we describe more briefly the period evolution for the other compounds. We shall in any case refer to the general period behaviour described for the thiobenzoate series: this general behaviour is characterized by a weak optical period near the low temperature phase transition, a period divergence (interpreted as a reversal) in the phase interval, and again a weak optical period near the high temperature phase transition [6]. Figure 4 displays the typical behaviour.

3.1. *First category: large SmC* temperature range/long aliphatic chain*

Numerous compounds belong to this category: $n = 11$ and 12 for the thiobenzoate series [6], two non-symmetric chiral dimesogens—10BP5TBB8* [7] and 12BP5BBP8* [8], and several benzoate esters—8HH, 9HH, 10HH, 11HF, 12HF, 9FH, 10FH, 11FF and 12FF. We shall now report results for one of them, 12HF, which exhibits behaviour typical of this first category.

Figure 1 displays the helical pitch evolution for the SmC^*_A and SmC* phases. In SmC^*_A, the pitch is about 0.42 µm, and does not vary. The liquid crystal displays selective reflection colours: it is red.

In the SmC* phase, the pitch is about 0.35 µm from 75°C to 98°C. It decreases slowly to 0.31 µm at 99.5°C, and falls from 0.31 to 0.2 µm between 99.5°C and 100.5°C. The liquid crystal is green on the plateau ($\lambda = np$) and

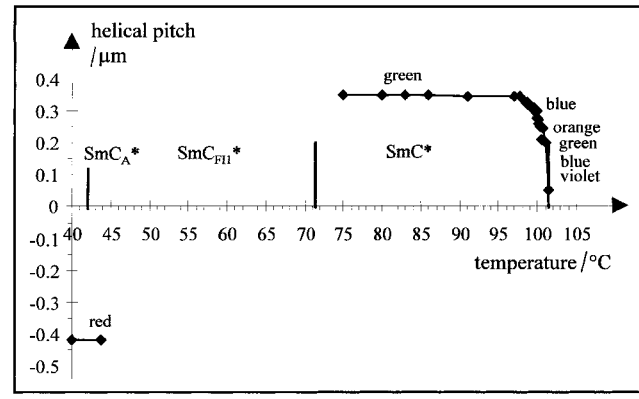

Figure 1. Helical pitch versus temperature, in the SmC^*_A and SmC* phases, for compound 12HF.

becomes blue, violet ($\lambda = np$) and red, orange, green, blue, violet ($\lambda = 2np$) during the pitch fall. As with the thiobenzoate series, the analysis of the selectively reflected circular light shows that the double helices occurring in the SmC^*_A phase and the SmC* phase helix exhibit opposite twist signs.

Figure 2 displays the optical period evolution versus temperature in SmC^*_α. As for the thiobenzoate series, we plot the double optical period versus temperature.

On heating, the period exhibits only the high temperature part of the general behaviour. The SmC*–SmC^*_α transition occurs at 99.5°C ①. The Friedel fringes are already tightened at the transition and go on tightening when the temperature increases; they move apart just before the transition to the SmA phase (101.6°C): the double period decreases from 0.18 µm at 99.5°C to 0.09 µm at 101°C ②. It then increases ③ up to 0.18 µm at 101.6 ④.

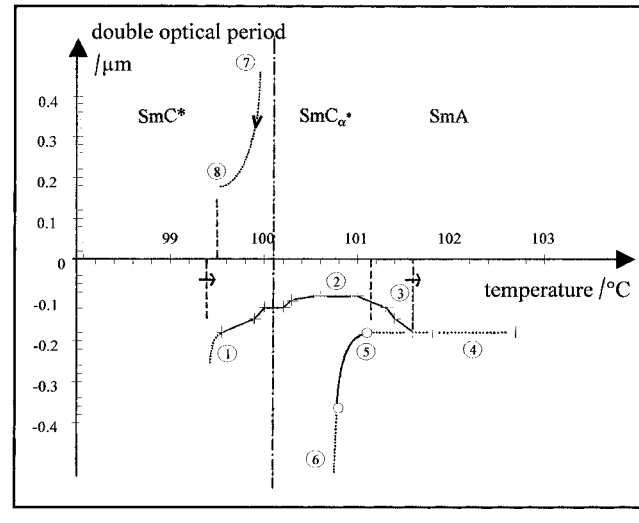

Figure 2. Double optical period versus temperature in the SmC^*_α phase for compound 12HF; on heating (+) from the SmC* phase, and on cooling from the SmA phase (○).

On cooling, the complete general behaviour is observed. In the SmA phase, the fringes are blurred and motionless. They move again at 101.1°C, indicating the SmA—SmC$^*_\alpha$ transition ⑤. The double period then increases from 0.18 to 0.36 μm at 100.8°C, and reverses at about 100.5°C ⑥. After the reversal, new fringes appear ⑦ and tighten, but no measurement could be performed. Still tightening, the fringes become violet ($\lambda = 2np$) at 99.5°C: this reveals the transition to the SmC* phase ⑧.

3.2. *Second category: SmC* short temperature range/intermediate length of aliphatic chain*

Three compounds belong to the second category: $n = 10$ for the thiobenzoate series, and 9FF and 10FF for the benzoate series. For the SmC$^*_A$ and SmC* phases, we report the pitch behaviour only for the 9FF compound. In SmC$^*_\alpha$, two different behaviours can occur: we therefore report results for the 9FF and 10FF compounds.

Figure 3 displays the pitch variation in the SmC$^*_A$ and SmC* phases for 9FF. The pitch evolution is similar to that observed for the 12HF compound, except near the SmC*–SmC$^*_\alpha$ transition: the transition occurs at 90.8°C with a discontinuity, and no pitch fall is observed. The pitch values are also bigger than for 12HF: about 0.66 μm in the SmC$^*_A$ phase and 0.45 μm on the plateau in the SmC* phase.

In SmC$^*_\alpha$, for both compounds, the Friedel fringes form on heating in the transition front. They are very tightened just after the transition, and move apart when the temperature increases; two evolutions can then be observed. Figure 4 shows the double period evolution for the 9FF compound. We observed the complete general behaviour: the transition occurs at 87.9°C ①, with a front crossing the sample. The double optical period decreases suddenly, reaching 0.06 μm at 89°C ②. It then increases ② – ③ and reverses ③ – ④, and decreases again ⑤ – ⑥. This evolution is reversible, ⑥ – ⑦ – ⑨ – ⑩.

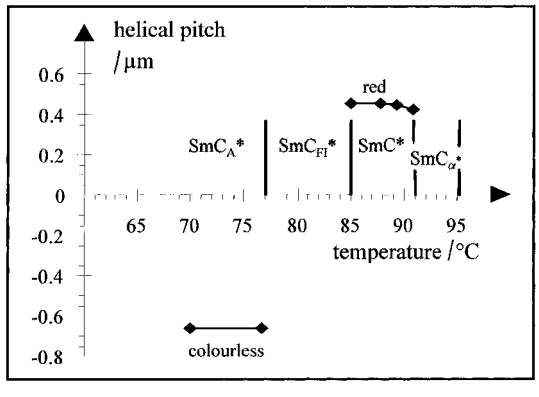

Figure 3. Helical pitch versus temperature in the SmC$^*_A$ and SmC* phases for compound 9FF.

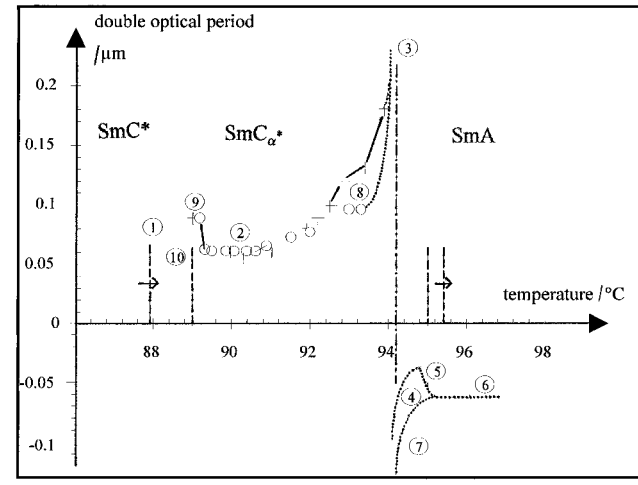

Figure 4. Double optical period versus temperature in the SmC$^*_\alpha$ phase for compound 9FF; on heating (+) from the SmC* phase, and on cooling from the SmA phase (○).

Figure 5 displays the period evolution for the 10FF compound. The period follows only the low temperature part of the general behaviour: it decreases just after the transition ① – ②, and then increases regularly ② – ③ with neither divergence nor reversal. On cooling, the period is a little bigger, but displays the same evolution ④ – ⑤ – ⑥.

3.3. *Third category: no SmC* phase in the sequence/short aliphatic chain*

Among the benzoate compounds, only 8FH belongs to the third category, but other compounds of different series belong to this classification: one non-symmetric chiral dimesogen (10BP5TBB9*), $n = 9$ for the thiobenzoate series. On some samples of compound $n = 10$ (thiobenzoate series) the SmC* phase disappears from the sequence. In this case, we observe a direct SmC$^*_{FI}$–SmC$^*_\alpha$ transition, and the compound also belongs to this third category [6].

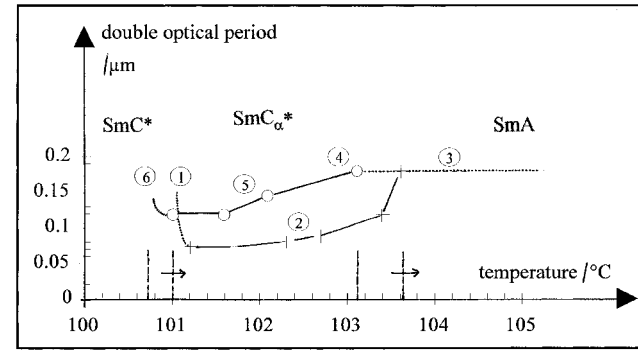

Figure 5. Double optical period versus temperature in the SmC$^*_\alpha$ phase for compound 10FF; on heating (+) from the SmC* phase, and on cooling from the SmA phase (○).

The 8FH compound does not exhibit SmC* or SmC^*_{FI2}. We thus observe a direct SmC^*_{FI1}–SmC^*_α transition: the defects observed in the SmC^*_{FI1} phase transform into fringes in SmC^*_α. The evolution of the fringe period depends on the low temperature phases formed before. This influence has been previously described for a thiobenzoate series [6].

Figures 6(*a*) and 6(*b*) display the optical period evolution versus temperature on cooling from the SmA phase, and on heating, respectively, from the SmC^*_{FI1} and SmC^*_A phases.

On cooling from SmA, we always observe the complete general behaviour. The reversal occurs at a high temperature (about 100.5°C), close to the SmA–SmC^*_α transition.

On heating in the SmC^*_{FI1} phase (figure 6(*a*)—the SmC^*_A phase has not been reached on cooling) the defects are motionless. They are very tightened, their double period being about 0.05 µm ①. They move apart between 97.8 and 98°C ②, and transform into fringes, that reveal the transition to SmC^*_α ②; the fringe period could not be measured. The sample then follows the complete general behaviour, the reversal ②–③ occurring at low temperature, just after the transition.

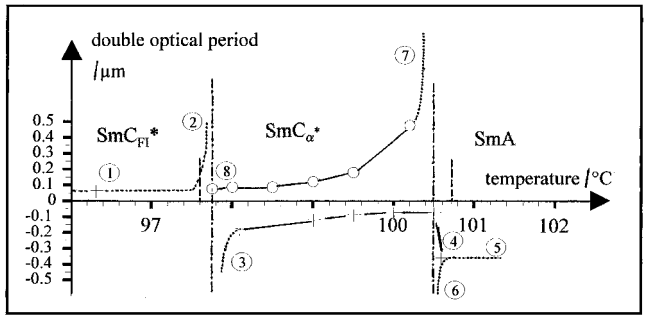

(*a*)

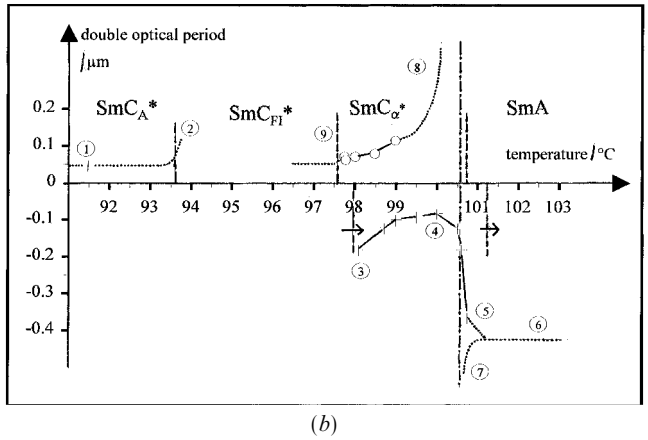

(*b*)

Figure 6. Double optical period versus temperature in the SmC^*_α phase for compound 8FH: (*a*) on heating (+) from the SmC^*_{FI1} phase, and on cooling from the SmA phase (○); (*b*) on heating (+) from the SmC^*_A phase, and on cooling from the SmA phase (○).

On heating from the SmC^*_A phase, figure 6(*b*), the SmC^*_A defects are in this case very tightened—their double period is about 0.06 µm ①. When heating, the defects move apart at the SmC^*_A–SmC^*_{FI1} transition, at 93.6°C ②. In the SmC^*_{FI1} phase, the defects continue to move, and their period seems to be significant at high temperature. The transition to SmC^*_α occurs with a front crossing the sample; the period is already reversed in SmC^*_α ③. It follows only the high temperature part of the general behaviour ③–④–⑤–⑥.

3.4. *An unusual phase sequence: the compound 10HF*

Observation of the compound 10HF in a prismatic cell in the SmC* phase shows that the helical pitch is about 0.6 µm and does not vary. On heating, approaching the SmC^*_α phase, each Grandjean–Cano thread splits into two threads. This phenomenon is usually observed in the SmC* phase, close to a SmC^*_{FI} phase. Figure 7 shows this on a free surface drop of 10HF on heating.

On a free surface drop, we observed between the SmC* and SmC^*_α phases a texture similar to that of a SmC^*_{FI} phase: this 'new phase' appears over 2°C on heating and about 11°C on cooling. The SmC^*_{FI}–SmC^*_α transition occurs with a discontinuity, but the Friedel fringes seem to transform into SmC^*_{FI} defects. Figures 8 and 9 show a 10HF drop exhibiting, respectively, the SmC^*_α texture (in the SmC^*_α phase) and the SmC^*_{FI} texture.

This unusual phase could not be detected using other experimental techniques, and evidence for it is very difficult to obtain on a free surface drop. Such a sequence 'SmC*–SmC^*_{FI}–SmC^*_α' has been previously observed and described for a chiral non-symmetric dimesogen (10BB5BBB8*) [8]. In both cases, the SmC^*_{FI} and SmC^*_A phases do not appear at low temperature in the sequence, and the SmC^*_α phase occurs over a large temperature range, about 10°C. Both series also include benzoate cores.

Figure 10 displays the optical period evolution for 10HF. On heating, the period decreases slightly at the transition, increases regularly (2–3–4) with neither reversal nor divergence. This behaviour is reversible with temperature (5–6–7). It must be pointed out that the 10HF compound in fact exhibits the second category behaviour, with a short SmC* phase and the low part of the general behaviour in the SmC^*_α phase.

4. Discussion

We shall now try to correlate the optical period evolution in the SmC^*_α phase with the phase difference α, in the SmC^*_α domain and in the low temperature phase, close to the transition to the SmC^*_α phase. We

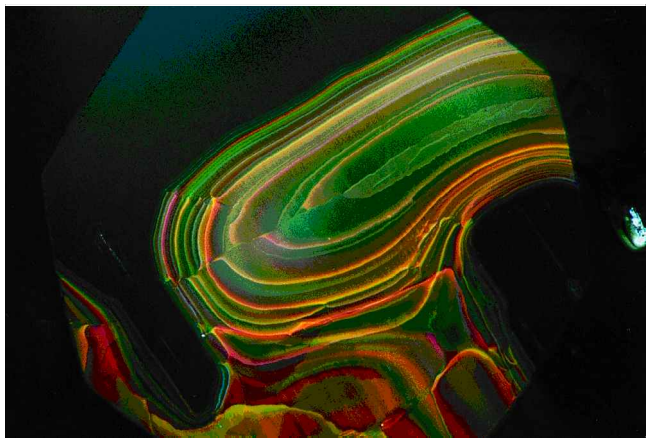

Figure 7. Compound HF10 as a free surface drop at 73.2°C in the SmC* phase close to the SmC*–SmC$^*_\alpha$ transition. On heating, the Grandjean-Cano threads split into two threads.

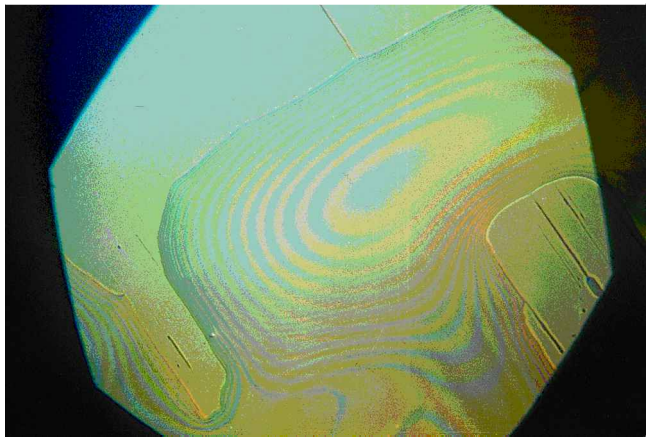

Figure 8. Compound HF10 in SmC$^*_\alpha$ phase at 76.4°C. The sample exhibits Friedel fringes, the characteristic SmC$^*_\alpha$ texture.

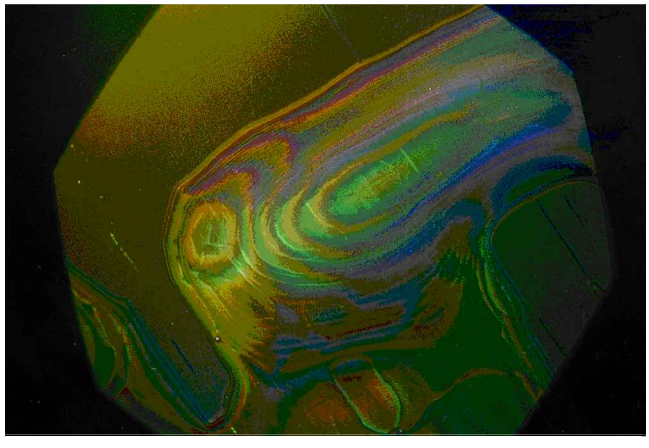

Figure 9. Compound HF10 on cooling from the SmC$^*_\alpha$ phase at 66.3°C. The sample exhibits the SmC$^*_{FI}$ texture with characteristic grey SmC$^*_{FI}$ defects.

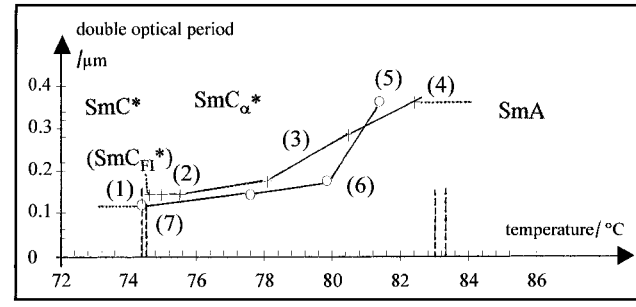

Figure 10. Double optical period versus temperature in the SmC$^*_\alpha$ phase for compound 10HF; on heating (+) from the SmC* phase and on cooling from the SmA phase (○).

shall establish this correlation for each category and relate it to the structure proposed by Zeks and Cepic for the SmC$^*_\alpha$ phase [4, 5]. For the first category the helical pitch in SmC* is almost constant over a large temperature interval, and falls at the SmC*–SmC$^*_\alpha$ transition from a value ranging between 0.6 and 0.35 to 0.13 μm (violet, $\lambda = 2np$). At the transition, the azimuthal angle difference α is thus significant (higher than 11° for $p = 0.13\,\mu m$ and a layer thickness of 40 Å). When the transition occurs, α can thus rapidly reach and cross $\pi/2$. When we observe the Friedel fringes in the SmC$^*_\alpha$ phase, the period divergence has already occurred. We observe only the high temperature part of the general behaviour in which $\alpha > \pi/2$.

For the second category the pitch in SmC* is significant, and no fall is observed at the SmC*–SmC$^*_\alpha$ transition. At the transition, α is still weak (about 3° for $p = 0.45\,\mu m$); it can thus increase in the SmC$^*_\alpha$ phase and can cross $\pi/2$ several degrees after the transition. If the SmC$^*_\alpha$ domain is large, we observe the whole general behaviour; if the domain is narrow, the SmC$^*_\alpha$–SmA transition occurs before α reaches $\pi/2$. We observe only the low temperature part of the general behaviour, without any divergence.

For the third category (direct SmC$^*_{FI}$–SmC$^*_\alpha$ transition) the period evolution is imposed by the period of the SmC$^*_{FI}$ defects, and probably by the azimuthal angle difference in SmC$^*_{FI}$, close to the transition. If α is smaller than $\pi/2$, it can increase and cross $\pi/2$ in the SmC$^*_\alpha$ domain; we thus observe the whole general behaviour. If α is bigger than $\pi/2$ in SmC$^*_{FI}$, it ranges between $\pi/2$ and π in the SmC$^*_\alpha$ domain, and we observe only the high temperature part of the general behaviour.

For the fourth category (the unusual phase sequence), we observed the SmC$^*_{FI}$ texture, between typical SmC* and SmC$^*_\alpha$ textures. We wonder if it is really an additional phase in the sequence or if it corresponds to a particular texture of the SmC$^*_\alpha$ phase. This phase indeed occurs over a large temperature range; the tilt angle is thus probably significant at low temperatures, and the

azimuthal angle is also significant. These conditions are somewhat similar to those observed for a real SmC^*_{FI} phase and could generate the same type of texture.

5. Conclusion

The structural model proposed by Zeks and Cepic allows us to interpret qualitatively the optical period values and their evolution in the SmC^*_α temperature domain. The SmC^*_α phase exhibits a helical structure, with a significant phase difference α that increases with temperature and can cross $\pi/2$. This value of α and the fluctuations measured by Farhi and Nguyen [11] for the tilt angle in SmC^*_α can explain the fragility of the phase structure: when α increases, the molecular interactions decrease. The absence of strong molecular interactions prevents structure stabilization and makes it very sensitive to any fluctuation of initial conditions or temperature. Besides, for $\alpha = \pi/2$, the optical period diverges; weak α variations around $\pi/2$ then produce very significant period variations. The dispersion is then amplified, so favouring the observation of several behaviours for the same phase. The structural fragility appears in our experimental study in these different period evolutions, and also in other ways: the Friedel fringes can display different evolutions at different places in the same sample and a hysteresis is frequently observed (the period divergence occurs at different temperatures on cooling and on heating).

A study performed by Mach *et al.* [12, 13] on free-standing films, using resonant X-ray diffraction at the sulphur K-edge, confirms the SmC^*_α structure—the so-called 'clock model'. According to this study, the superlattice period (corresponding to the helical pitch) ranges in the SmC^*_α phase between 5 and 8 smectic layers. This conclusion is in qualitative agreement with our study. A calculation is now in process in our laboratory [14] to determine the correlation between the optical period, the azimuthal difference, and the helical pitch. First estimations of the helical pitches deduced from our optical period measurements are consistent with the value obtained by Mach *et al.*

References

[1] Nguyen, H. T., Rouillon, J. C., Cluzeau, P., Sigaud, G., Destrade, C., and Isaert, N., 1994, *Liq. Cryst.*, **17,** 571.
[2] Brunet, M., and Isaert, N., 1988, *Ferroelectrics*, **84,** 25.
[3] Laux, V., Isaert, N., Nguyen, H. T., Cluzeau, P., and Destrade, C., 1996, *Ferroelectrics*, **179,** 25.
[4] Zeks, B., and Cepic, M., 1993, *Liq. Cryst.*, **14,** 445.
[5] Cepic, M., and Zeks, B., 1995, *Mol. Cryst. liq. Cryst.*, **263,** 61.
[6] Laux, V., Isaert, N., Nguyen, G., and Joly, G., 1999, *Liq. Cryst.*, **26,** 361.
[7] Faye, V., Nguyen, H. T., Laux, V., and Isaert, N., 1996, *Ferroelectrics*, **179,** 9.
[8] Faye, V., Babeau, A., Placin, F., Nguyen, H. T., Barois, P., Laux, V., and Isaert, N., 1996, *Liq. Cryst.*, **21,** 485.
[9] Laux, V., 1997, PhD thesis, Université de Lille I, France, n° 2076 (unpublished).
[10] Faye, V., Rouillon, J. C., Destrade, C., and Nguyen, H. T., *Liq. Cryst.*, **19,** 47.
[11] Farhi, R., and Nguyen, H. T., 1997, *Europhys. Lett.*, **40,** 49.
[12] Mach, P., Pindak, R., Levelut, A.-M., Barois, P., Nguyen, H. T., Huang, C. C., and Furenlid, L., 1998, *Phys. Rev. Lett.*, **81,** 1015.
[13] Mach, P., Pindak, R., Levelut, A.-M., Barois, P., Nguyen, H. T., Baltes, H., Hird, M., Toyne K., Seed, A., Goodby, J. W., Huang, C. C., and Furenlid, L., 1999, *Phys. Rev.* (to be published).
[14] Dètrè, L., 1999, PhD thesis, Université de Lille I, France, n° 2398 (unpublished).